Revisiting two thiophosphate compounds constituting d^0 transition metal: HfP_2S_6 and d^{10} transition metal: α-$Ag_4P_2S_6$ as multifunctional materials for combining second harmonic generation response and photocurrent response

Craig Cropek [a, #], Bingheng Ji [a, #], Arka Sarkar [b], Fei Wang [c], Tajamul Hussain Syed [d], Wei Wei [d], Sheng-Ping Guo [e], Jian Wang [a] *

[a] *Department of Chemistry and Biochemistry, Wichita State University, Wichita, Kansas 67260, United States*

[b] *Department of Chemistry, Iowa State University, Ames, Iowa, 50011, United States*

[c] *Department of Chemistry, Missouri State University, Springfield, Missouri, 65897, United States*

[d] *Department of Mechanical Engineering, Wichita State University, Wichita, Kansas 67260, United States*

[e] *School of Chemistry and Chemical Engineering, Yangzhou University, Yangzhou, Jiangsu 225002, P. R. China*

[#] equally contributed.

Corresponding author: jian.wang@wichita.edu

Contents

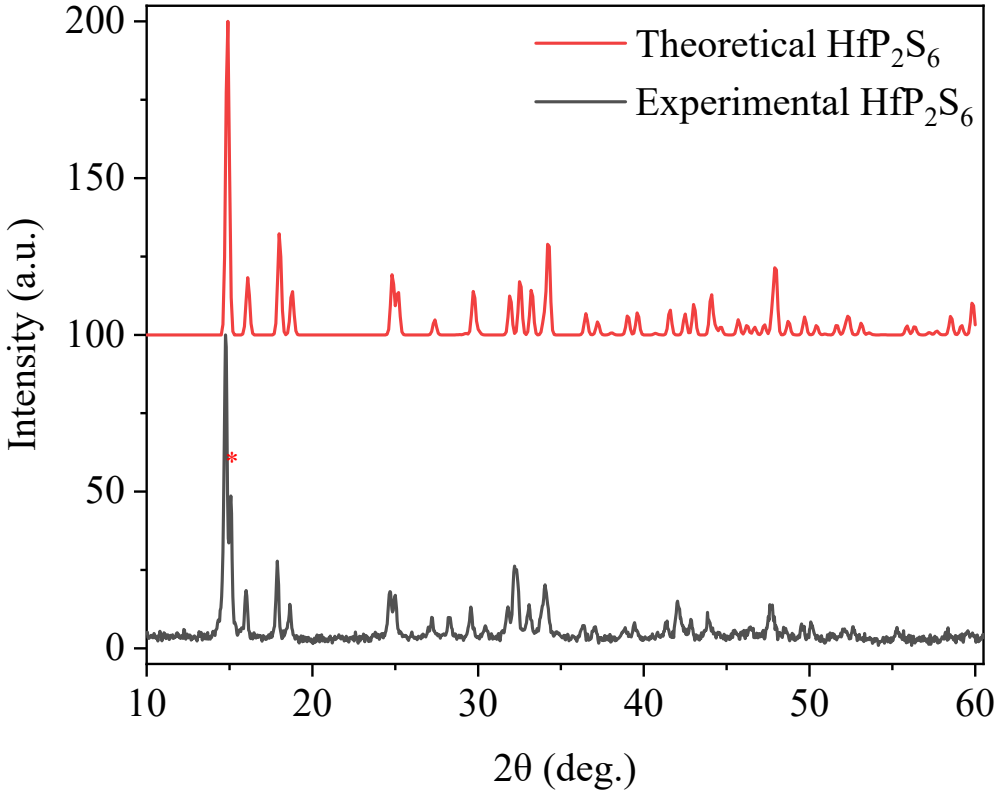

Figure S1. Theoretical and experimental powder XRD patterns of HfP_2S_6. The intrinsic impurity, HfS_2, is labeled as a red asterisk.

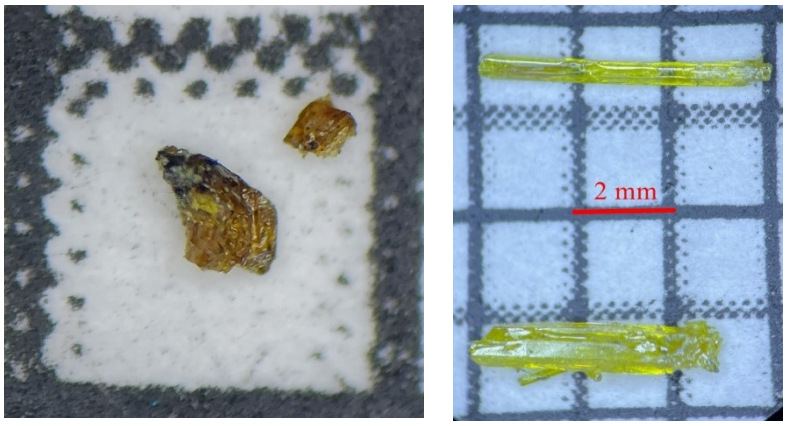

Figure S2. Optical microscope photos of selected crystals of HfP_2S_6 (left) and α-$Ag_4P_2S_6$ (right), the background is a 2 mm scale paper.

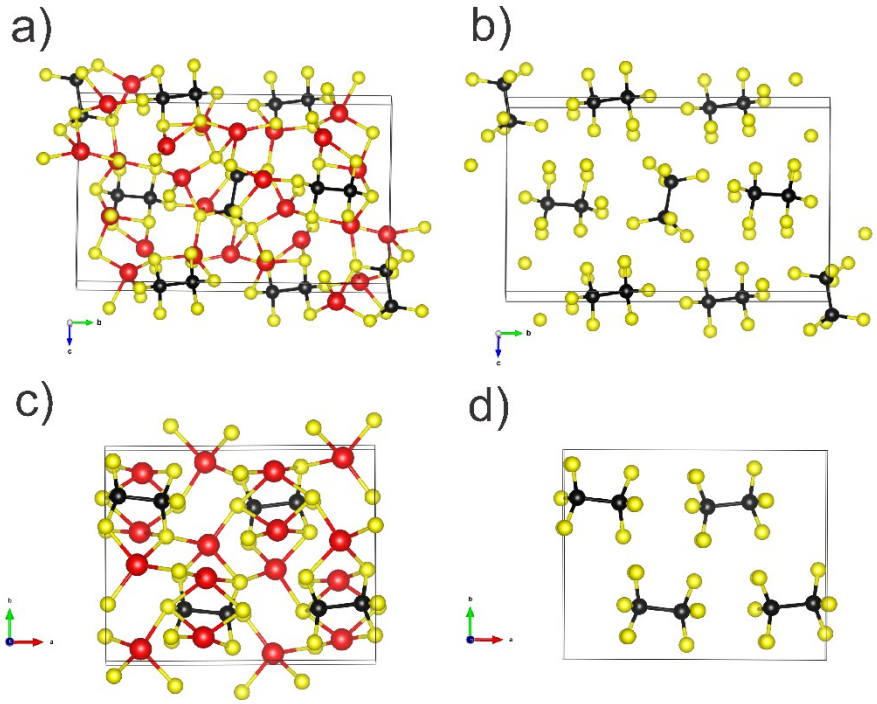

Figure S3. a) ball-stick model of β-$Ag_4P_2S_6$ viewed along [100] direction. b) The arrangement of [P_2S_6] motifs within β-$Ag_4P_2S_6$ viewed along [100] direction, Ag atoms are removed for clarity. c) ball-stick model of α-$Ag_4P_2S_6$ viewed along [001] direction. d) The arrangement of [P_2S_6] motifs within $Ag_4P_2S_6$ viewed along [001] direction, Ag atoms are removed for clarity. Ag: red color, P: black color, S: yellow color.

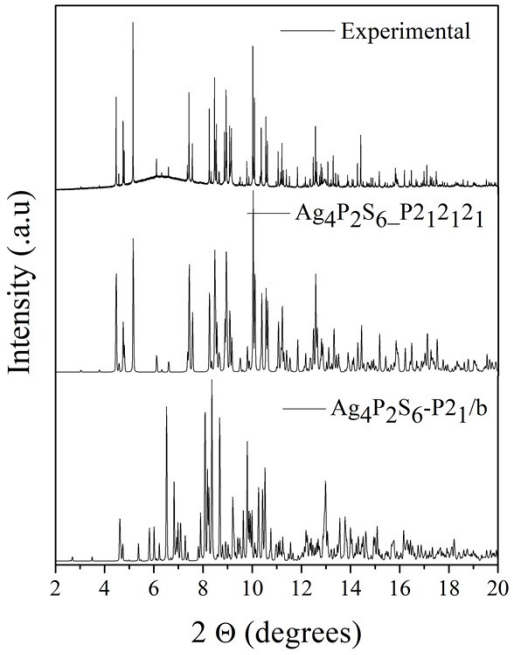

Figure S4. High resolution synchrotron X-ray diffraction results of α-$Ag_4P_2S_6$ together with two polymorphic simulated models.

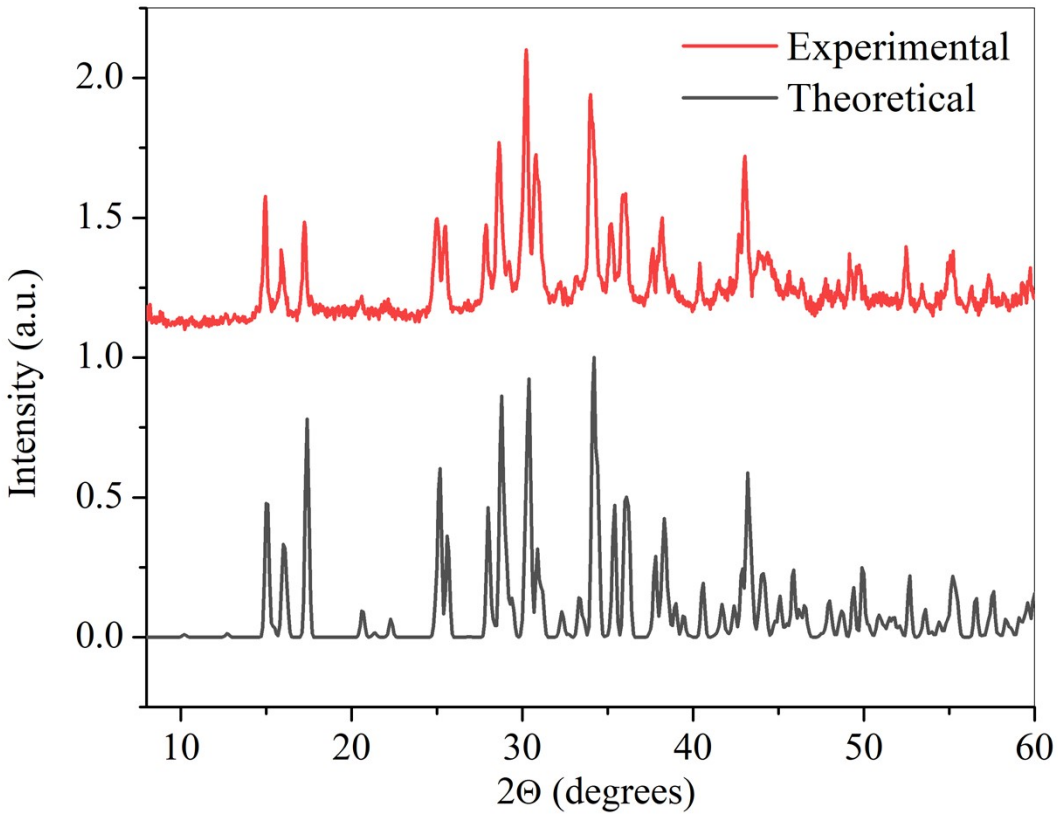

Figure S5. Lab powder X-ray diffraction results of α-$Ag_4P_2S_6$ together with theoretical pattern.

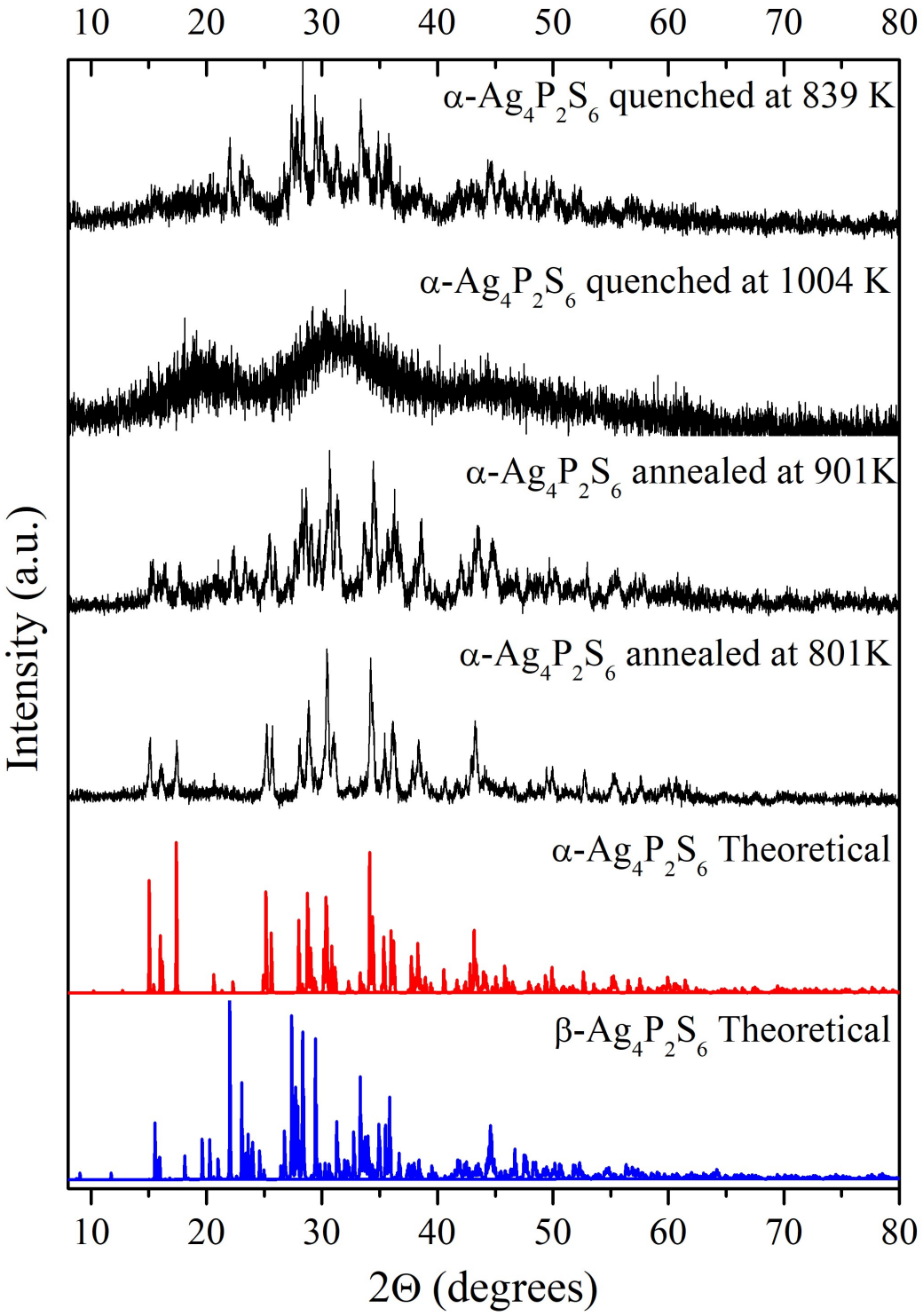

Figure S6. PXRD results of α-$Ag_4P_2S_6$ and β-$Ag_4P_2S_6$ samples after DSC treatments compared with theoretical patterns.

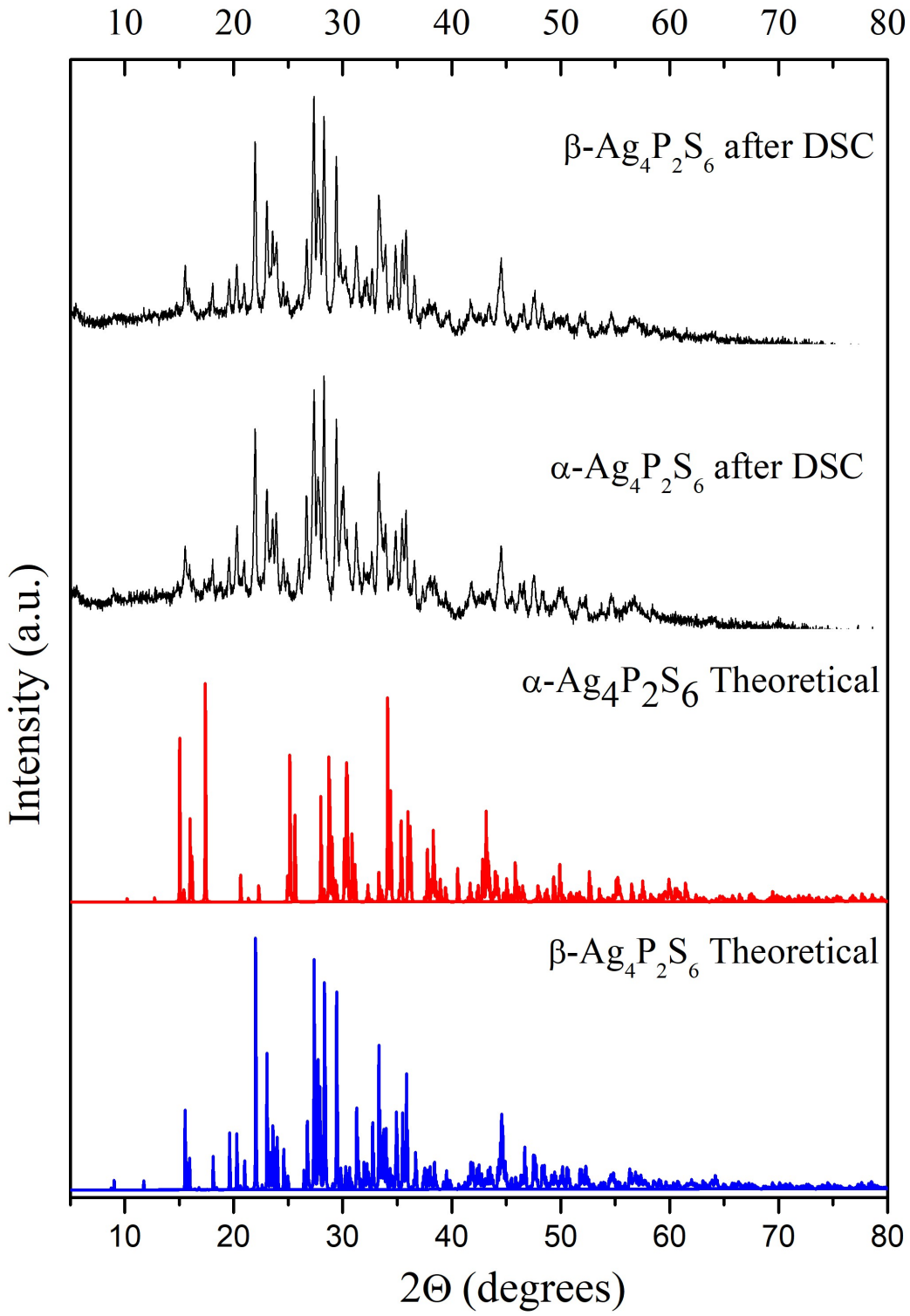

Figure S7. PXRD results of α-$Ag_4P_2S_6$ samples annealed and quenched at different temperatures. The theoretical patterns are listed at the bottom. The annealing process details: the target crystals were sealed and heated to the target temperature with holding for 10 hours and then quenched in

air. The quenching process detail: the target crystals were sealed and heated to 1173K first then cooled down to the target temperature and then quenched in iced water.

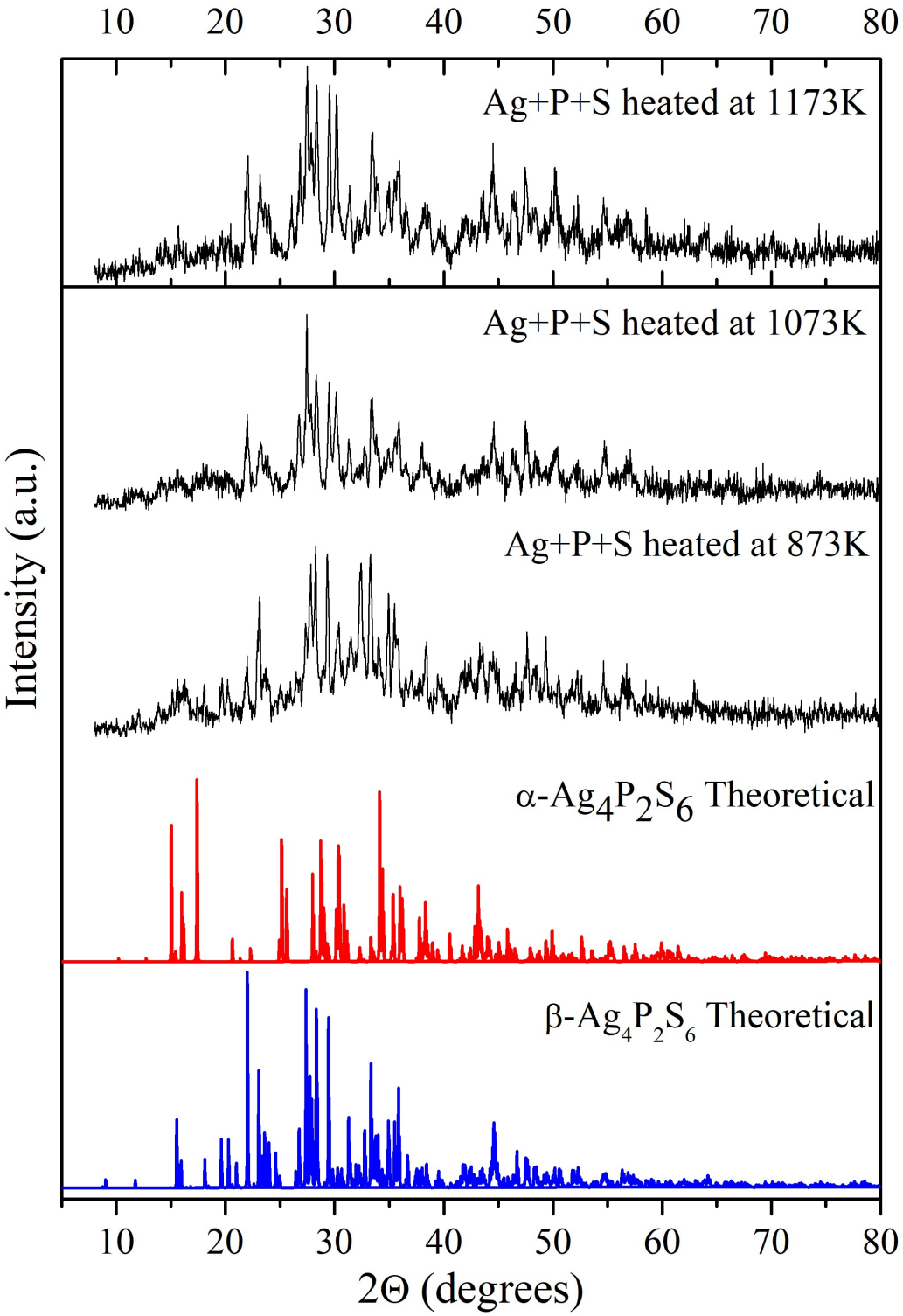

Figure S8. PXRD results of samples synthesized via heating Ag+P+S elements at different temperatures. The theoretical patterns are listed at the bottom.

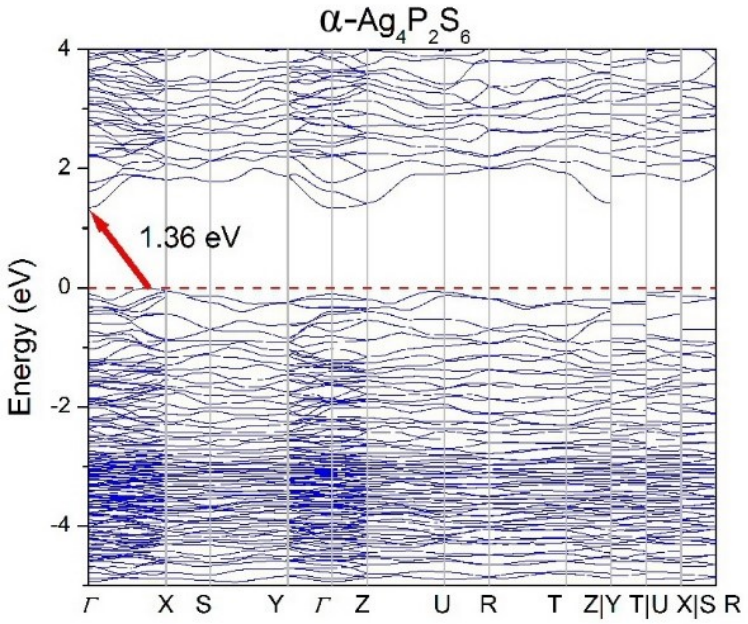

Figure S9. Calculated band structure of α-$Ag_4P_2S_6$ from VASP.

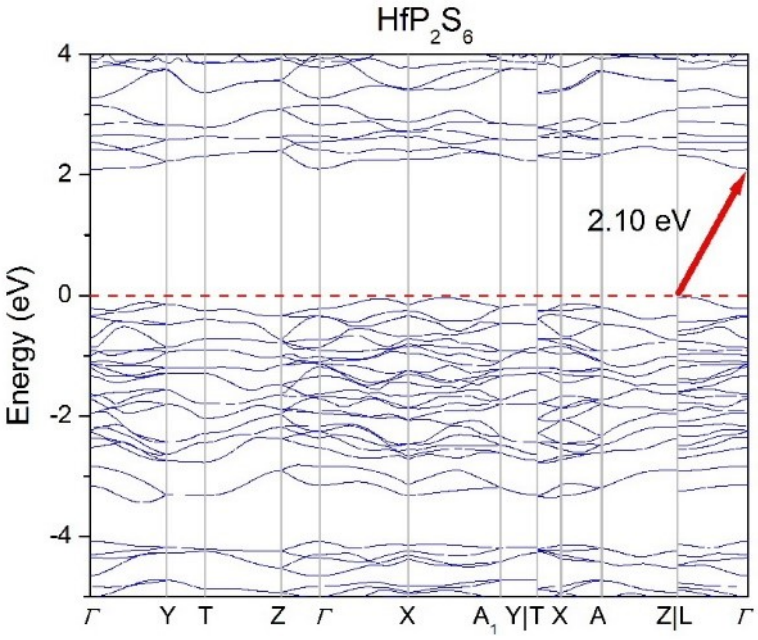

Figure S10. Calculated band structure of HfP_2S_6 from VASP.

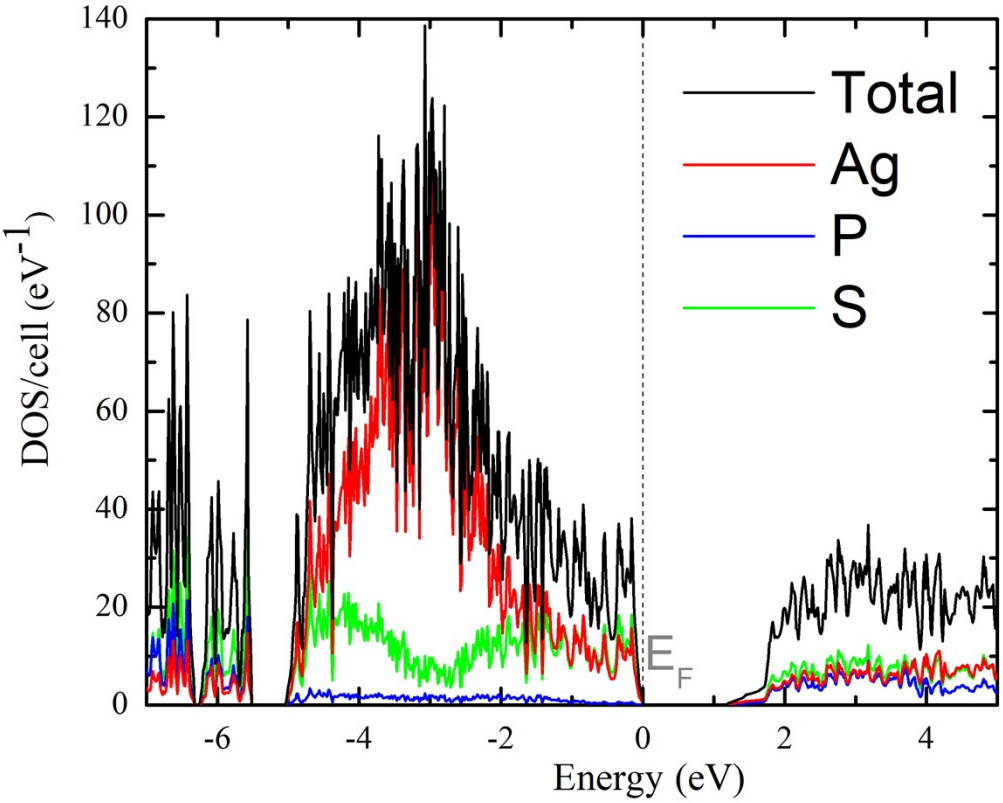

Figure S11. Density of states of α-$Ag_4P_2S_6$ calculated by TB-LMTO-ASA.

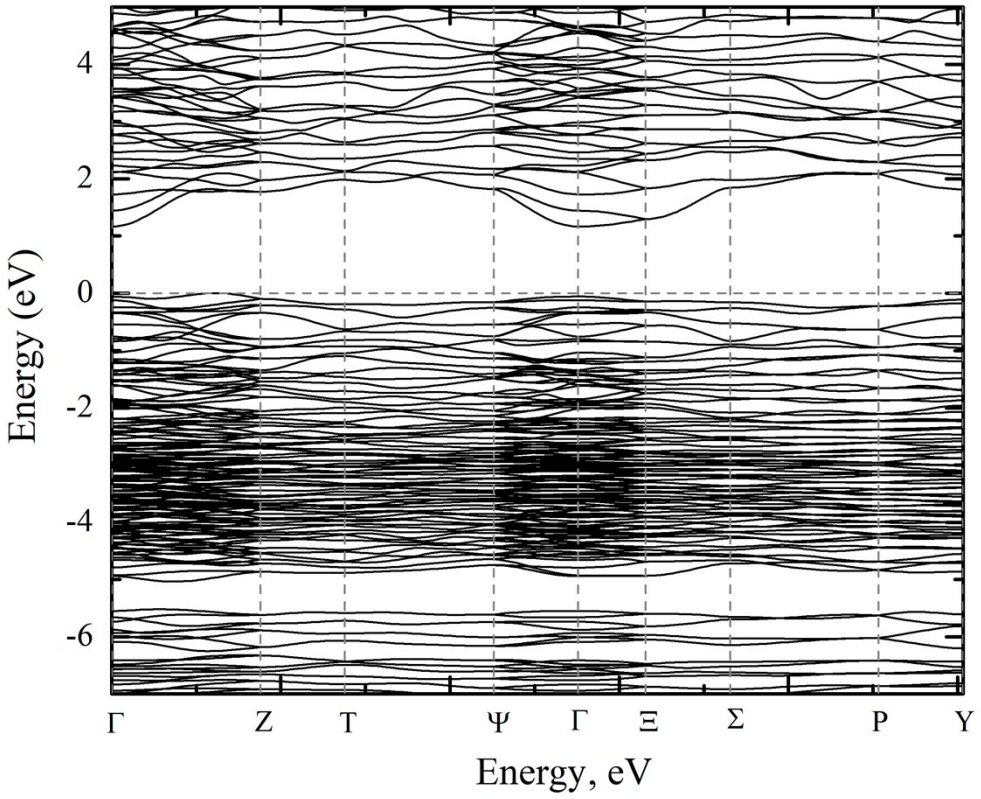

Figure S12. Band structure of α-$Ag_4P_2S_6$ calculated by TB-LMTO-ASA.

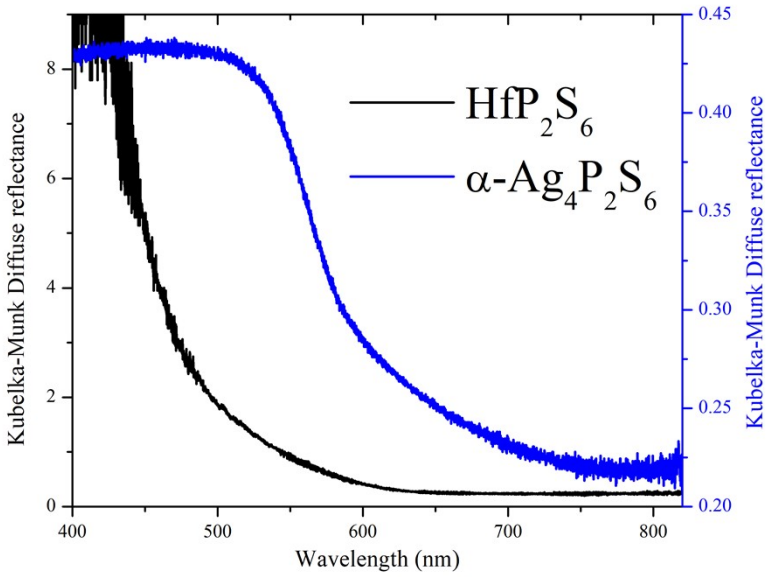

Figure S13. The Kubelka-Munk diffuse reflectance plots of HfP_2S_6 (black) and α-$Ag_4P_2S_6$ (blue).

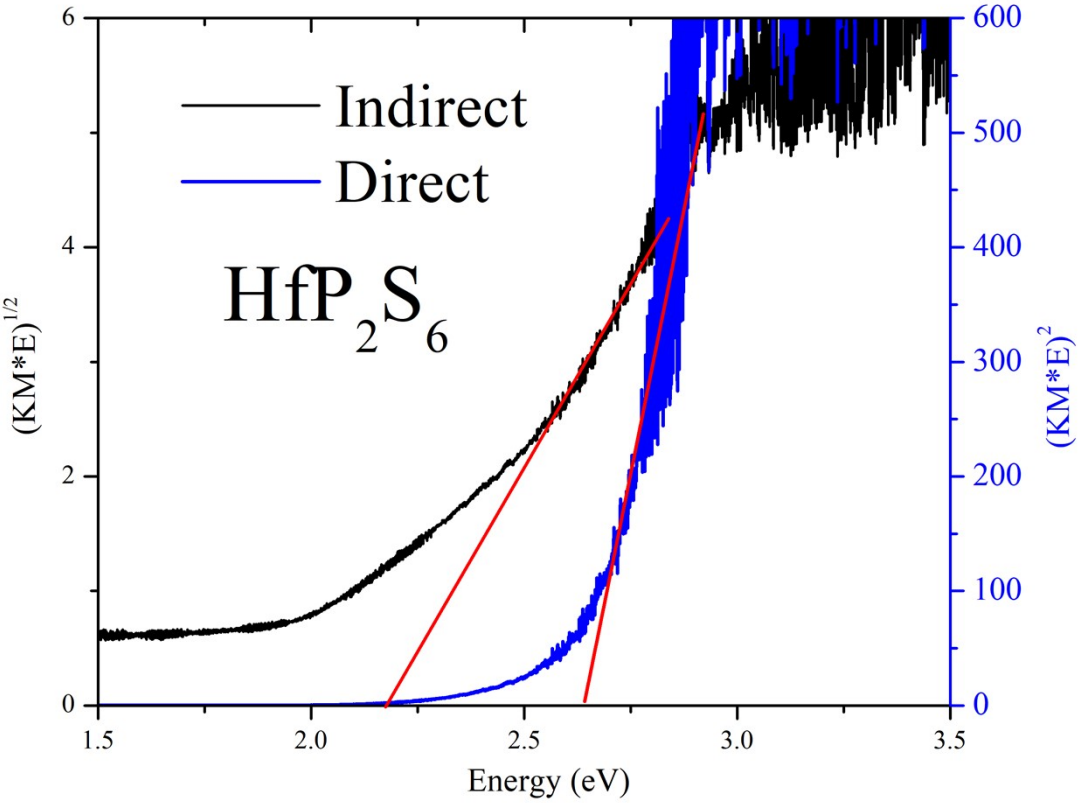

Figure S14. Tauc plots for allowed direct and indirect transitions of HfP_2S_6

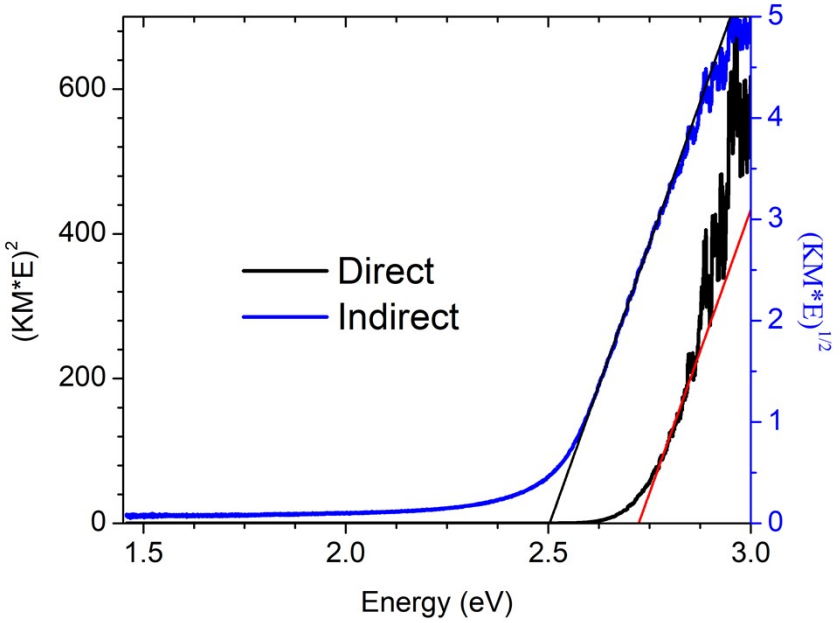

Figure S15. Tauc plots for allowed direct and indirect transitions of α-$Ag_4P_2S_6$.

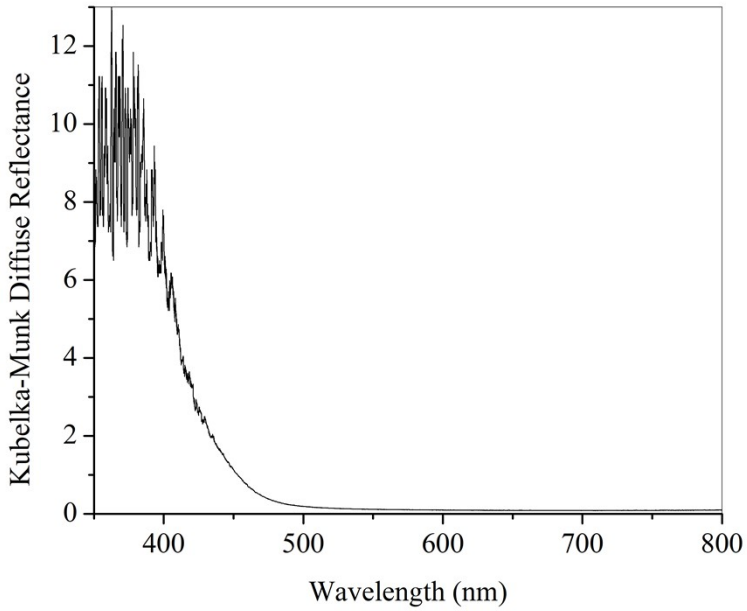

Figure S16. The Kubelka-Munk diffuse reflectance plots of β-$Ag_4P_2S_6$.

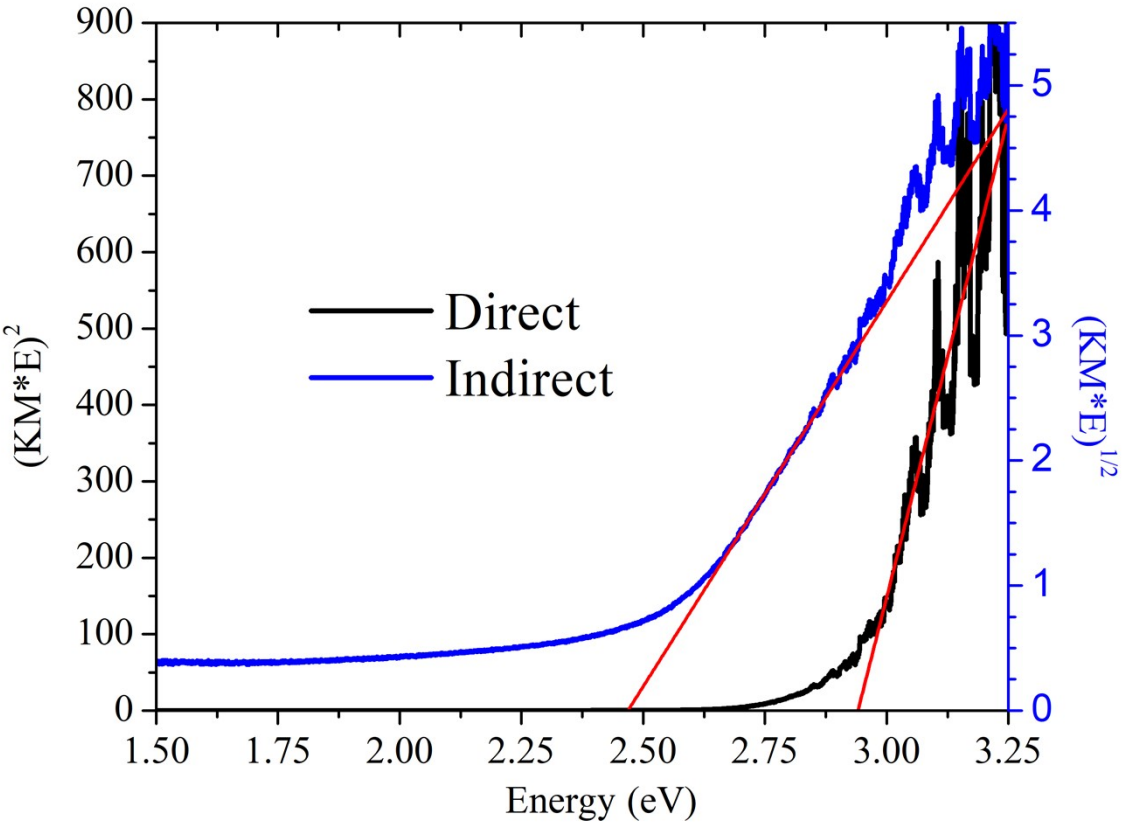

Figure S17. Tauc plots for allowed direct and indirect transitions of β-$Ag_4P_2S_6$.

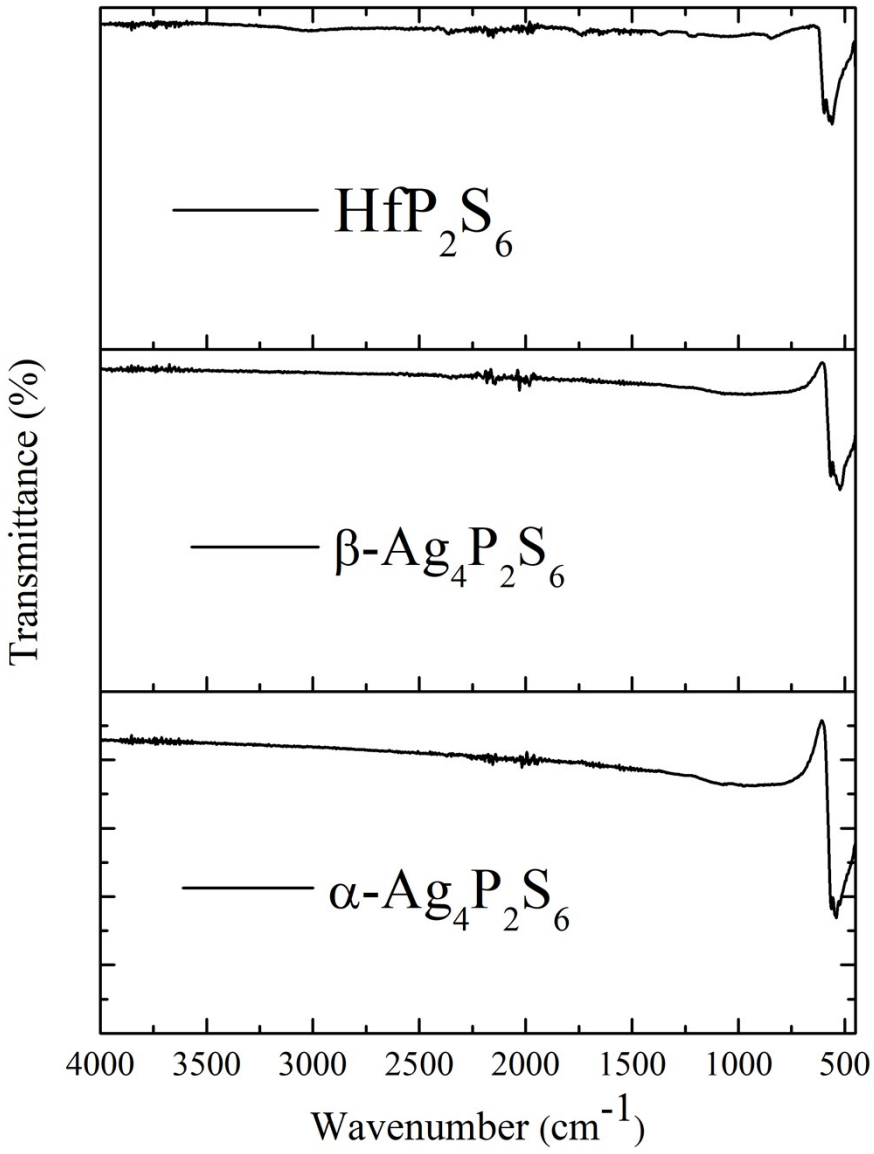

Figure S18. IR spectrum of HfP_2S_6, α-$Ag_4P_2S_6$, and β-$Ag_4P_2S_6$.

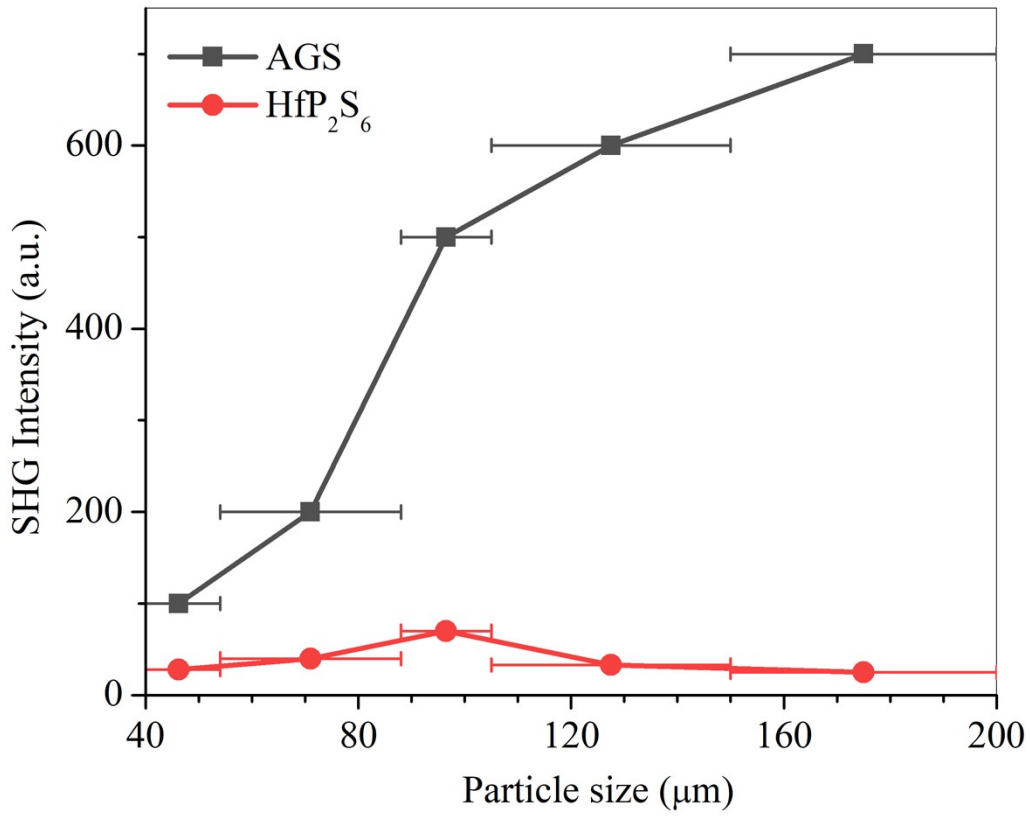

Figure S19. SHG intensities of HfP_2S_6 and $AgGaS_2$ were measured on variable particle size samples utilizing a 2.09 μm laser.

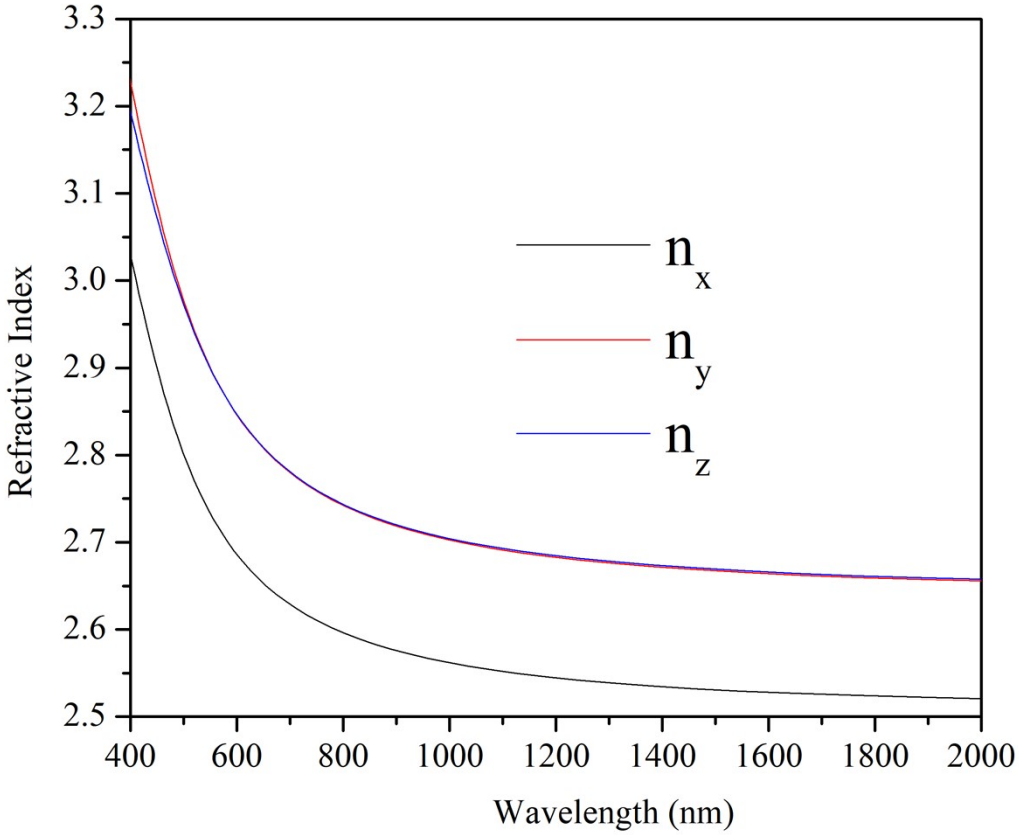

Figure S20. Calculated birefringence of α-$Ag_4P_2S_6$ versus wavelength of the fundamental light.

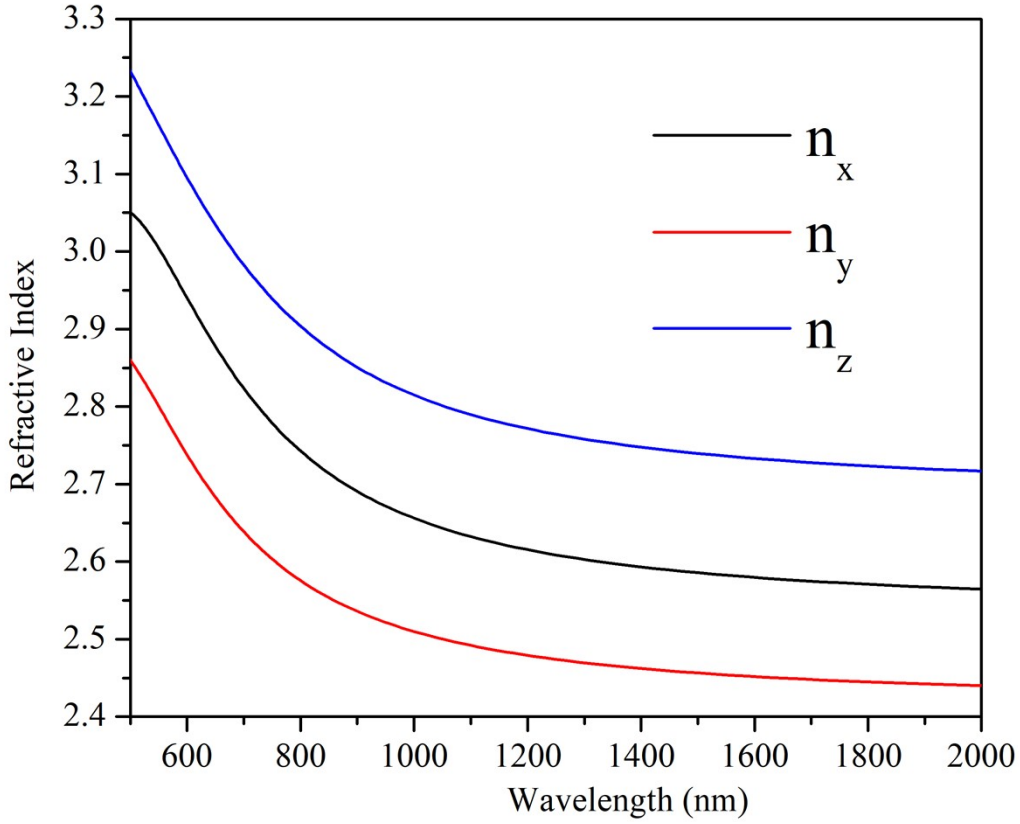

Figure S21. Calculated birefringence of HfP_2S_6 versus wavelength of the fundamental light.

Table S1. LDT measurement results of $Ag_4P_2S_6$ and $AgGaS_2$ @ 1064 nm measured at samples of particle size of 225 μm.

	damage energy (mJ)	**spot diameter (mm)**	**LDT (MW/cm^2)**	**LDT (× AGS)**
$AgGaS_2$	0.58	0.5	29.6	1
α-$Ag_4P_2S_6$	1.85	0.5	94	3.2

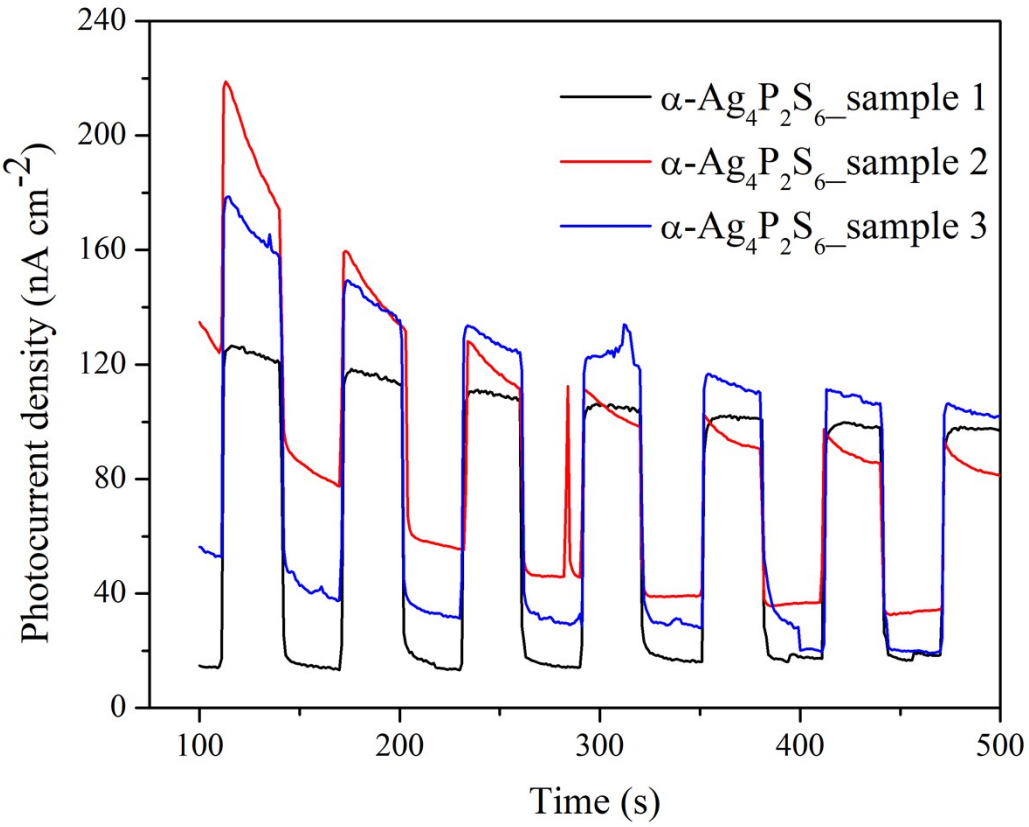

Figure S22. Photocurrent density of three samples of α-$Ag_4P_2S_6$.

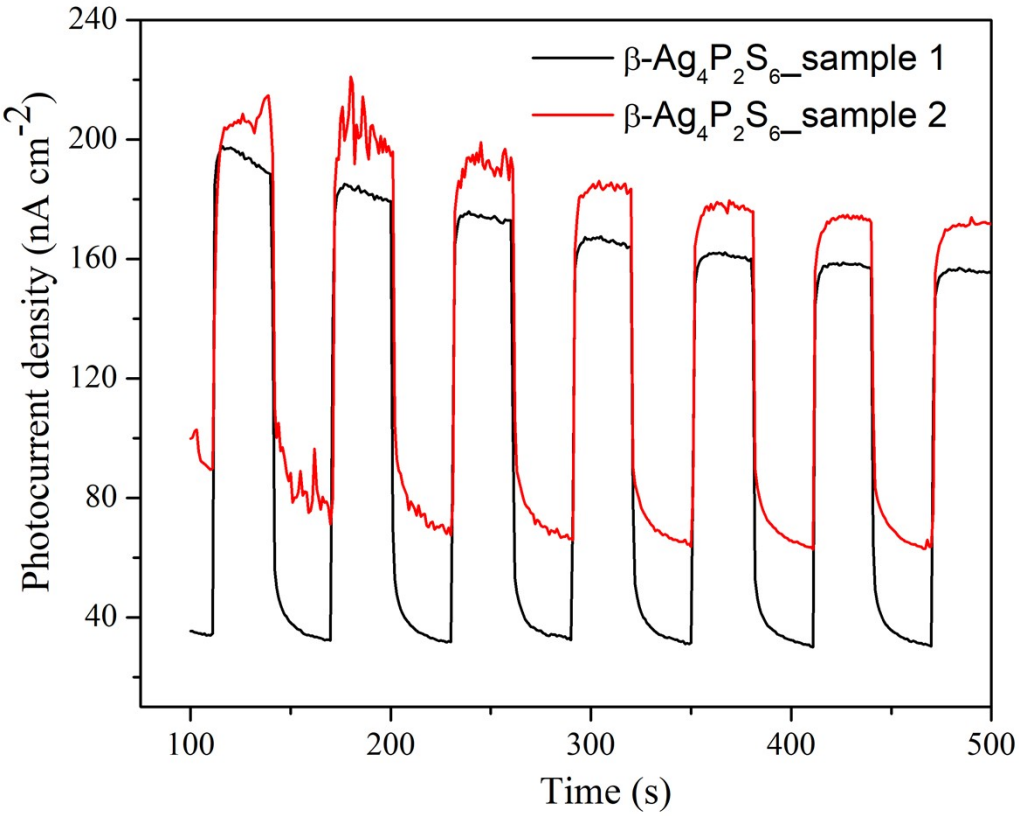

Figure S23. Photocurrent density of two samples of β-$Ag_4P_2S_6$.

Table S2. Photocurrent response of selected sulfides (ranked by photocurrent density from highest to lowest)

Compounds	Photocurrent density	References
$Ba_5Bi_2Co_2S_{10}$	4 mA cm^{-2}	1
KCu_2BiS_3	0.11 mA cm^{-2}	2
$Pb_3P_2S_8$	45 μA cm^{-2}	3
$Ba_3HgGa_2S_7$	12.2 μA cm^{-2}	4
$Rb_2CuSb_7S_{12}$	10 μA cm^{-2}	5
$Eu_8In_{17.33}S_{34}$	1 μA cm^{-2}	6
$CsCuS_4$	0.55 μA cm^{-2}	7
$SrCuSbS_3$	0.54 μA cm^{-2}	8
α-$Ag_4P_2S_6$	165 nA cm-2	This work
β-$Ag_4P_2S_6$	135 nA cm^{-2}	This work
$BaCuSbS_3$	55 nA cm^{-2}	9
$Cs_2Ag_2Zn_2S_4$	50 nA cm^{-2}	10
$Rb_2Ba_3Cu_2Sb_2S_{10}$	6 nA cm^{-2}	11
$TlHgInS_3$	0.35 nA cm^{-2}	12

References:

1. K. Bu, X. Zhang, J. Huang, M. Luo, C. Zheng, R. Wang, D. Wang, J. He, W. Zhao, X. Che and F. Huang, *Chem. Commun. (Camb.)*, 2019, **55**, 4809–4812.
2. G. Zhang, B. Zhang, H. Chen, X. Zhang, C. Zheng, J. Lin and F. Huang, *J. Alloys Compd.*, 2014, **591**, 6–10.
3. B. Ji, E. Guderjahn, K. Wu, T. H. Syed, W. Wei, B. Zhang and J. Wang, *Phys. Chem. Chem. Phys.*, 2021, **23**, 23696–23702.
4. X. Huang, S.-H. Yang, W. Liu and S.-P. Guo, *Inorg. Chem.*, 2022, **61**, 12954–12958.
5. Y. Xiao, S.-H. Zhou, R. Yu, Y. Shen, Z. Ma, H. Lin and Y. Liu, *Inorg. Chem.*, 2021, **60**, 9263–9267.
6. Y. Chi, T.-F. Jiang, H.-G. Xue and S.-P. Guo, *Inorg. Chem.*, 2019, **58**, 3574–3577.
7. Q.-N. Yan, B.-W. Liu, X.-M. Jiang, J.-X. Zhao, S.-M. Pei, W.-F. Chen and G.-C. Guo, *Dalton Trans.*, 2022, **51**, 5561–5566.
8. X. Zhang, J. He, R. Wang, K. Bu, J. Li, C. Zheng, J. Lin and F. Huang, *Sol. RRL*, 2018, **2**, 1800021.
9. . Liu, P. Hou, W. Chai, J. Tian, X. Zheng, Y. Shen, M. Zhi, C. Zhou and Y. Liu, *J. Alloys Compd.*, 2016, **679**, 420–425.
10. Y. Liu, D. Xuan, Z. Song, L. Geng, B. Zhang and T. Liu, *J. Solid State Chem.*, 2022, **315**, 123457.
11. C. Liu, Y. Xiao, H. Wang, W. Chai, X. Liu, D. Yan, H. Lin and Y. Liu, *Inorg. Chem.*, 2020, **59**, 1577–1581.
12. H. Li, C. D. Malliakas, F. Han, D. Y. Chung and M. G. Kanatzidis, *Chem. Mater.*, 2015, **27**, 5417–5424.